Supplementary Information

Toward Continuous Monitoring of Breath Biochemistry: A Paper-Based Wearable Sensor for Real-Time Hydrogen Peroxide Measurement in Simulated Breath

Daniela Maier,[†] Elmar Laubender,[†,‡] Abhiraj Basavanna,[†] Stefan Schumann,[§] Firat Güder,[∥] Gerald A. Urban,[†,⊥] and Can Dincer[*,†,‡,∥]

[†]Department of Microsystems Engineering (IMTEK), Laboratory for Sensors and [‡]Freiburg Center for Interactive Materials and Bioinspired Technologies (FIT), University of Freiburg, 79110 Freiburg, Germany

[§]Department of Anesthesiology and Critical Care, Medical Center - University of Freiburg, Faculty of Medicine, University of Freiburg, 79106 Freiburg, Germany

[∥]Department of Bioengineering, Imperial College London SW7 2AZ, London, United Kingdom

[⊥]Freiburg Materials Research Center (FMF), University of Freiburg, 79104 Freiburg, Germany

Correspondence to C.D.: dincer@imtek.de

Experimental Procedures

The chemicals and methods for the experiments are listed below. Unless otherwise stated, all chemicals were purchased from Sigma Aldrich, Germany.

- Humectants and electrolytes for sensor preparation
  - 1 M potassium chloride (KCl)
  - 0.1 M phosphate buffered saline (PBS) containing 0.1 M sodium chloride (NaCl)
  - 10× PBS: 1.37 M NaCl, 27 mM KCl in 0.1 M PBS
  - 1 M sodium acetate
  - 1 M ammonium acetate
  - 1 M monosodium phosphate
  - 10% glycerine in 1 M KCl (aqueous solution, also applies to the following solutions)
  - 10% ethylene glycol in in 1 M KCl
  - 10% polyethylene glycol (PEG) in 1 M KCl
- Hydrogen peroxide (30 wt%, Merck KGaA, Germany)
- 1 mM ferrocenemethanol for the electrochemical characterization of the paper based sensors

All electrochemical measurements in this work were performed with a potentiostat EmStat3 with an eight-channel multiplexer MUX8 and the corresponding software PSTrace 5.4 (PalmSens, The Netherlands).

Resolution of screen-printing

For assessing the limitation of screen printing, a mask with different structures for resolution testing was designed with CleWin (WieWeb software, The Netherlands) and ordered from Beta Layout GmbH (Germany). The test structures comprise lines with different widths (0.05 to 3 mm) and distances (0.05 to 1.5 mm), arrays of 3×3 circles with different diameters (0.05 to 3 mm) and squares of different edge lengths (0.05 to 3 mm), as illustrated in **Figure S1**. These structures were screen printed onto a paper substrate, by utilizing carbon paste (C2030519P4, Gwent Group, UK) and a squeegee. With this, the minimum width, realizable with this procedure, was determined. The smallest structures screen-printable were 100 µm thin lines, but their outcome was very inconsistent. In addition, 200 µm circles and squares, showed a uniform result, except that single lines of the array did not work for the 200 and 300 µm structures. These deficiencies might also stem from irregularities in the mask for such small structures. Therefore, structures with a width less than 300 µm were not considered further for electrode design.

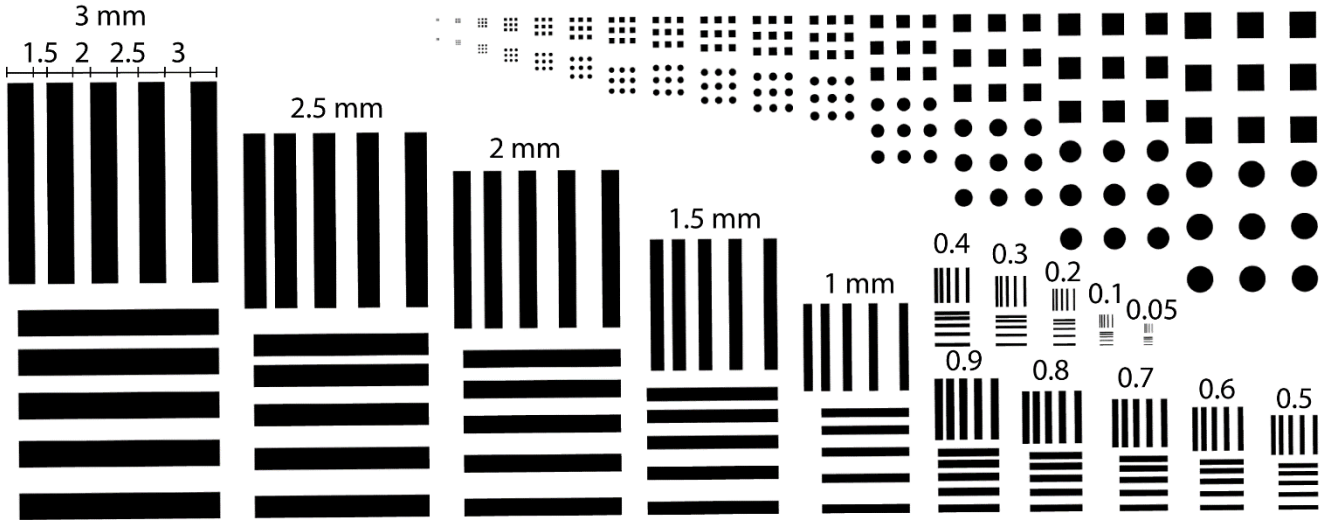

Figure S1. CAD drawing of structures used for resolution testing of screen-printing process, containing lines with different widths and distances (0.05 to 3 mm / 0.05 to 1.5 mm) and arrays of circles and squares with different diameters and edge lengths (0.05 to 3 mm).

Resistance measurements

To determine the minimum width with acceptable values for the conducting paths, resistance measurements were performed. As the voltage dependent current is gauged by amperometry, the resistance of the electrode structures has a huge impact on the sensor performance. Therefore, structures with different widths, as shown in **Figure S2**, were screen printed and their resistance was measured with the 4-point probes method.

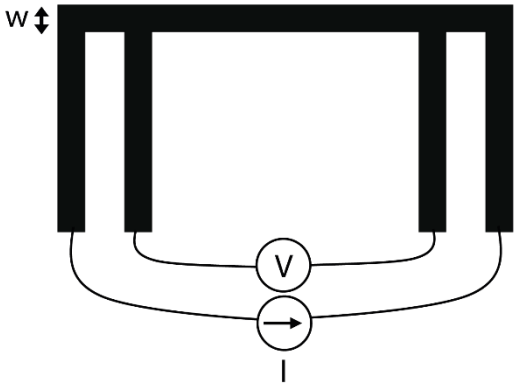

Figure S2. Scheme of structure and configuration for the resistance measurement with 4-point probes method to find the minimum width possible for the conducting paths. The current was applied to the outer legs and the voltage was measured at the inner legs of the structure.

Herein, carbon paste on paper and foil substrates, as well as the Prussian Blue (PB) and cobalt phthalocyanine (CP) mediated carbon pastes on paper were tested. In addition, the resistance of structures with silver / silver chloride beneath the carbon on paper were determined. The width of the measured structures ranged between 3 to 0.5 mm. The resulting resistances for structures with different materials and different widths are summarized in **Table S1**.

Table S1. Mean values of resistances for screen-printed structures with different widths and materials.

	Mean value of resistance in Ω							
Width in mm	3	2.5	2	1.5	1	0.9	0.2	
Carbon on paper	261.2 ± 45	296.8 ± 55	385.8 ± 52	477.4 ± 56	765.2 ± 127	843.2 ± 108	1477.0 ± 285	n = 5
Carbon on foil	228.3 ± 6	276.7 ± 16	375.7 ± 42	475.0 ± 58	682.0 ± 60	769.0 ± 83	1372.0 ± 48	n = 3
PB mediated carbon on paper	294.3 ± 46	313.7 ± 29	358.0 ± 17	465.7 ± 28	691.0 ± 35	820.0 ± 135	1345.0 ± 75	n = 3
CP mediated carbon on paper	242.7 ± 23	267.7 ± 6	306.3 ± 11	420.3 ± 32	662.7 ± 52	818.3 ± 147	1414.3 ± 320	n = 3
Ag/AgCl tracks beneath carbon on paper	0.07 ± 0	0.08 ± 0.01	0.1 ± 0	0.12 ± 0.02	0.19 ± 0.02	0.20 ± 0.01	0.50 ± 0.06	n = 3

As expected, the resistance of the structures increases with increasing width due to:

$$R = \rho \cdot \frac{l}{A}$$

With the electrical resistivity ρ, the length of the conductor l and the cross-sectional area A [1], which in composed of the width and the height h of the structure:

$$A = w \cdot h$$

Due to the high resistivity of the carbon pastes, the resistance was fairly high for the width of 1 mm preferred for the final chip design. Additional silver/silver chloride tracks were printed beneath the carbon tracks in order to decrease the resulting resistance. This width was chosen due to good results of the resolution test and as it offers an optimal size for a compact chip design.

Evaluation of different electrode designs

Two different electrode shapes, with the same 2D area, but different edge lengths, resulting in a different 3D area, were designed and fabricated. The idea was to assess the influence of the edge area on the current signal, as a larger overall area should lead to a higher signal. The two chip designs with differently shaped working electrodes are depicted in **Figure S3**. The bend electrode (design 2, **Figure S3B**) has a larger edge area, which is 1.55-times bigger than the round electrode (design 1, **Figure S3A**). Please note that the electrode height on the paper is presumed to be the same on a rigid substrate and taken from the product datasheet of the manufacturer.

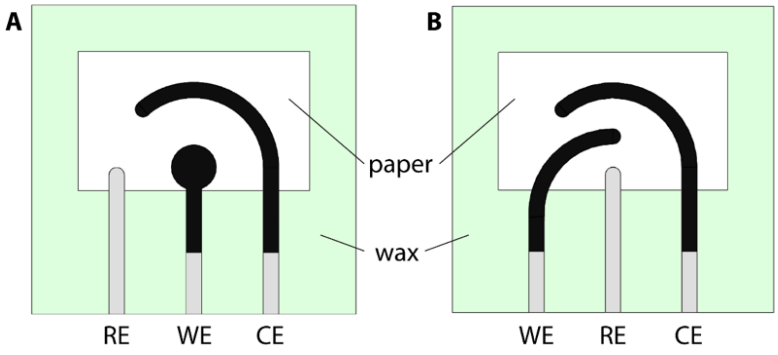

Figure S3. CAD drawings of two tested electrode designs with the same 2D area. Electrode design 1 **(A)** with a smaller edge area, compared to design 2 **(B)**. The paper window constitutes the electrochemical cell, where the electrolyte droplet is placed for the measurements. The wax isolation prevents the electrolyte to spread all over the sensor.

To determine a suitable voltage for the amperometric signal readout, previously multi-step amperometry was performed in 0.1 M PBS and 35.28 µM H_2O_2 in the range between −0.2 and 0.9 V with 50 mV steps. These results are illustrated in **Figure S4A-C** and show that the carbon paste shows no reaction to H_2O_2 in a potential range from −0.1 to 0.45 V *versus* Ag/AgCl (0.1 M PBS). For PB, a voltage of 0 V and for CP, 0.4 V were chosen as at these potentials highest current signals for H_2O_2, compared to PBS, were obtained.

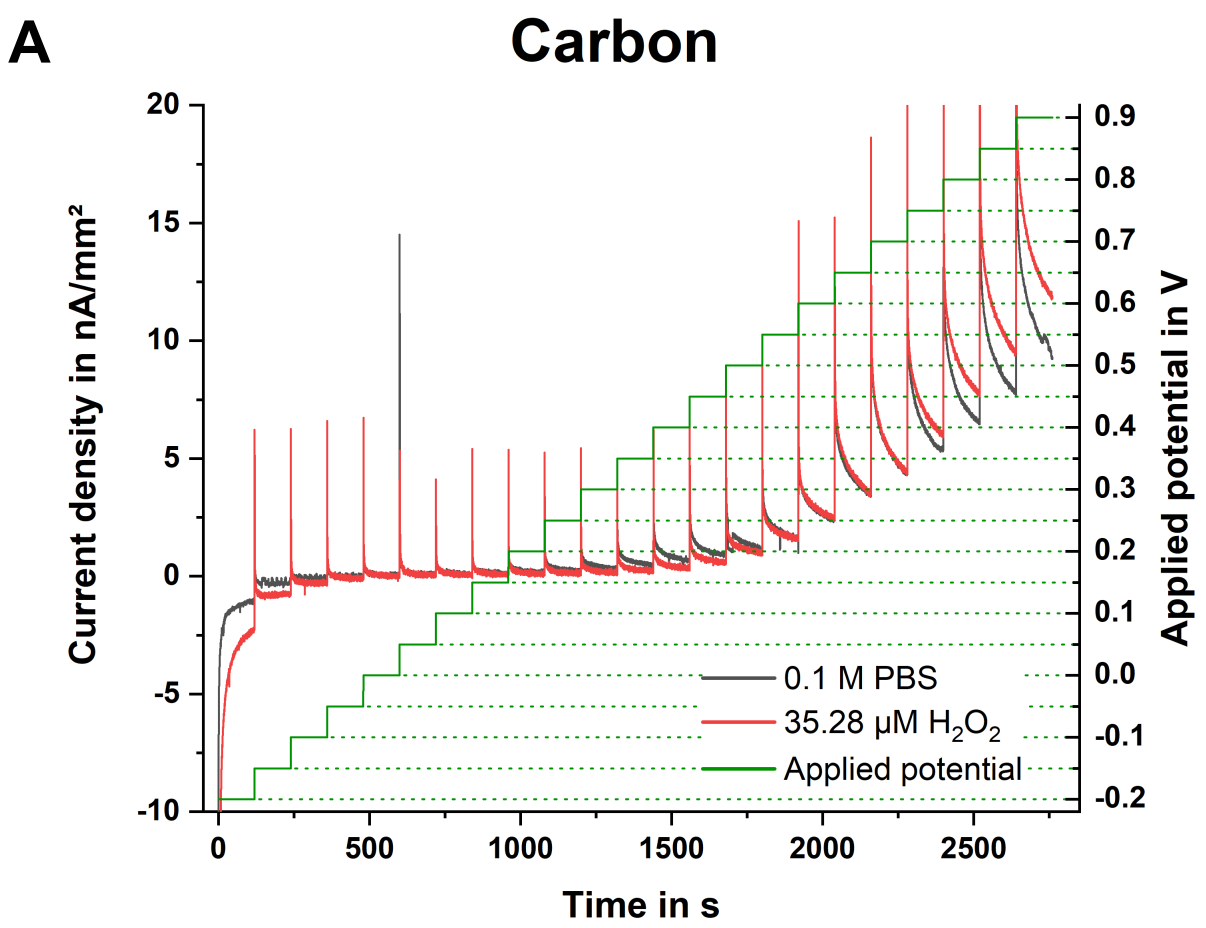
A
Carbon
Current density in nA/mm²
Applied potential in V
Time in s
0.1 M PBS
35.28 µM H2O2
Applied potential

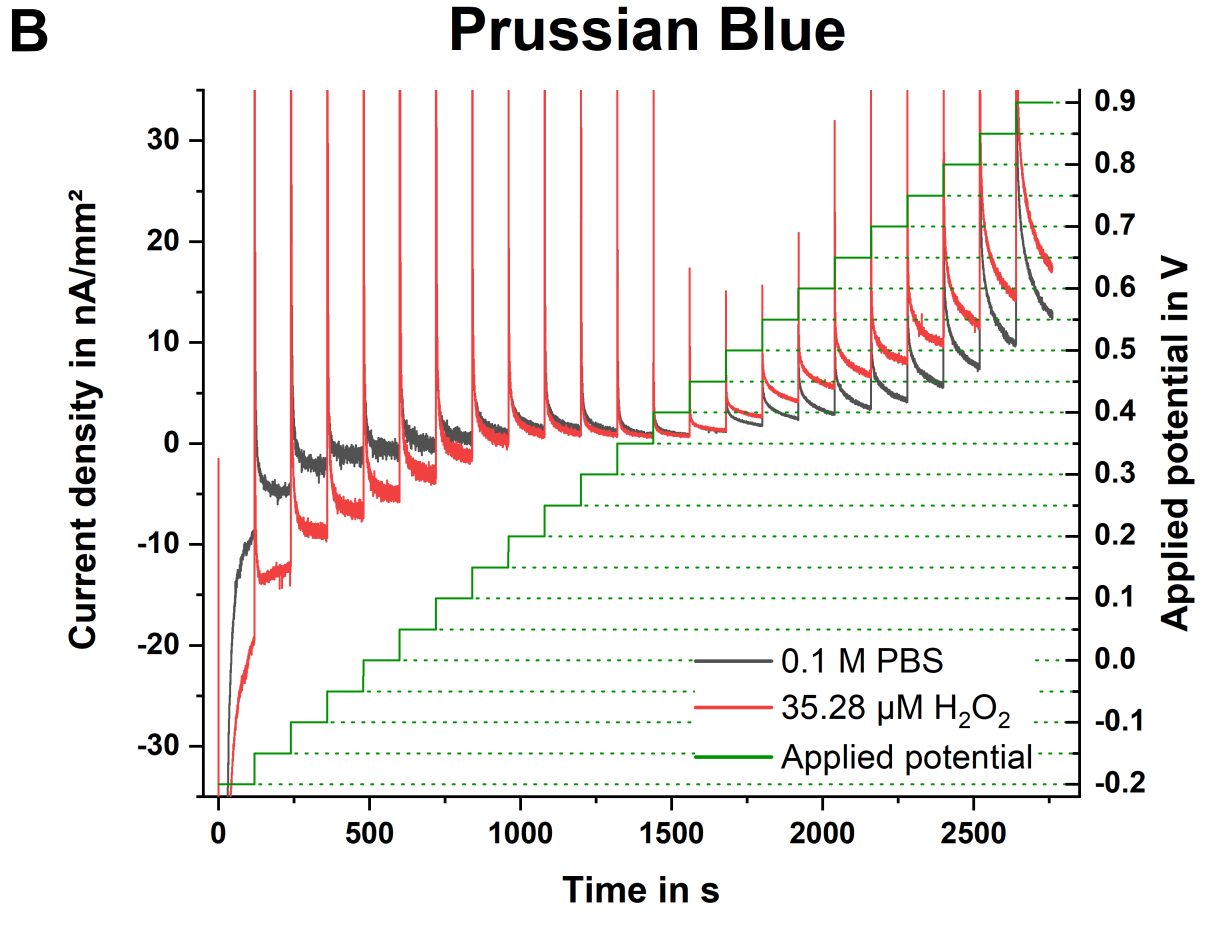
B
Prussian Blue
Current density in nA/mm²
Applied potential in V
Time in s
0.1 M PBS
35.28 µM H2O2
Applied potential

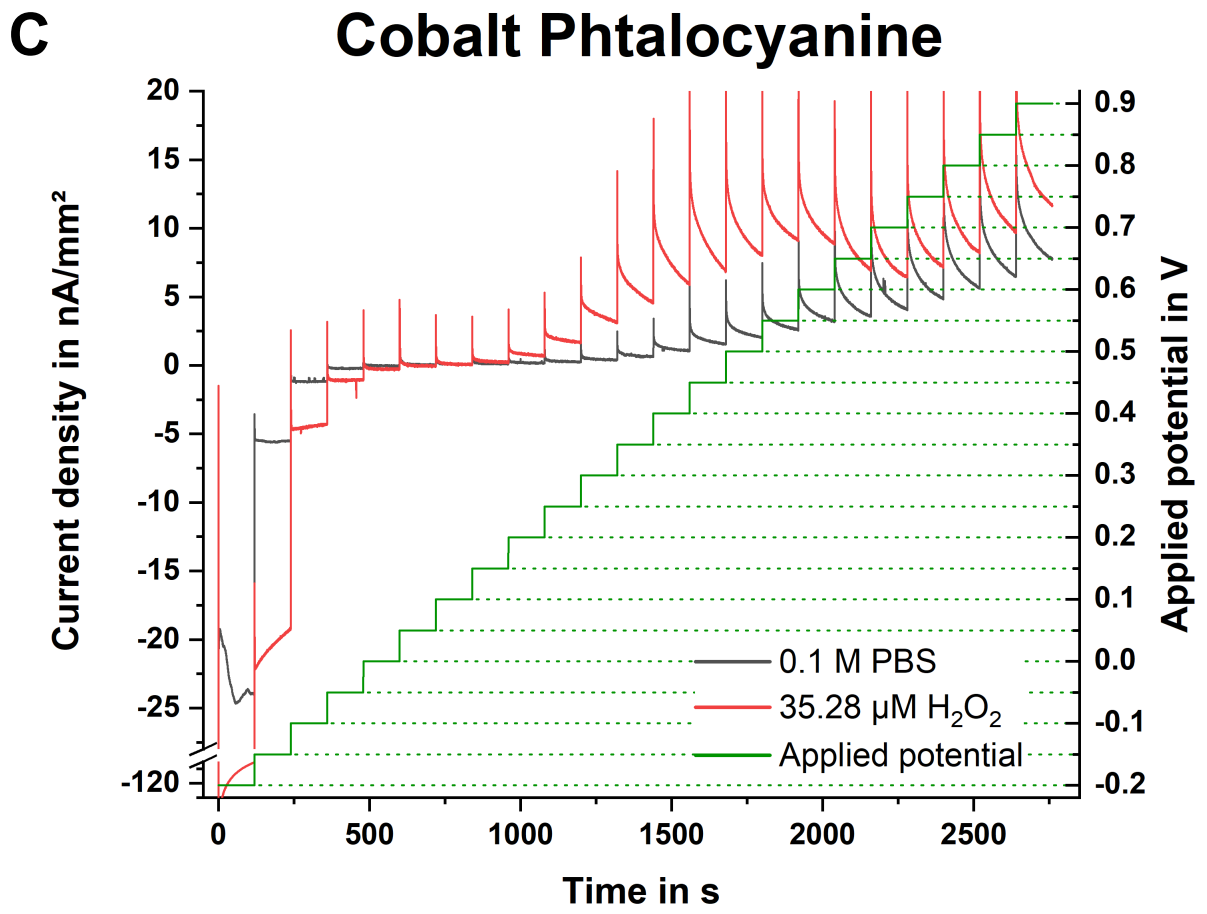

Figure S4. Results of multi-step amperometry for **(A)** carbon, **(B)** PB and **(C)** CP mediated carbon electrodes in 0.1 M PBS and 35 µM H_2O_2 at voltages in the range from -0.2 to 0.45 V vs. Ag/AgCl in 0.05 V steps. For PB and CP mediated electrodes, the highest signal difference between 0.1 M PBS and measured H_2O_2 concentration was observed at a voltage of 0.0 and 0.4 V, respectively. In the case of the carbon electrode, there was no significant signal change for H_2O_2 at the voltages of interest.

To compare the two designs, calibration curves of H_2O_2 were taken by means of amperometry using CP and PB mediated electrodes. Herein, the current signals for different H_2O_2 concentrations at a constant voltage of 0.0 V for PB and 0.4 V for CP were recorded. The calibration curves with the resulting mean current densities are illustrated in **Figure S5**. The CP paste proved to deliver lower current densities than the PB paste. The sensitivity for the CP paste was 0.053 and 0.041 nA μM^{-1} mm^{-2} with correlation coefficients of 0.99 for design 1 and 2, respectively. In the case of the PB mediated paste, the sensitivities were 0.12 and 0.16 nA μM^{-1} mm^{-2} with correlation coefficients of 0.99 for design 1 and 2, *vice versa*. In the case of PB, the curved structure (design 2) of the working electrode results in higher current densities as the diffusion of the analyte is enhanced at the edges by using such an electrode design compared to the circular one. Surprisingly, this was not the case for the CP paste which might be caused by the inappropriate assumption of the electrode height on the paper substrate.

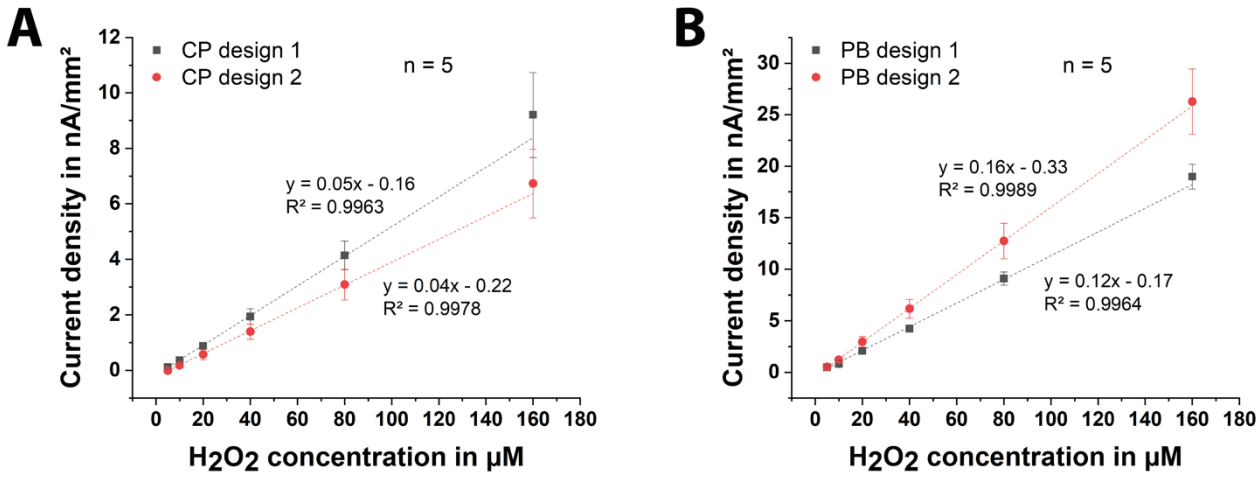

Figure S5. Calibration curves of different electrode designs with **(A)** CP and **(B)** PB mediated paste for different H_2O_2 concentrations. For the CP mediated paste, design 1 had the higher sensitivity, compared to design 2. Overall, the best results were achieved with PB, where design 2 had the highest sensitivity. Error bars represent ± SD of n = 5 replicates.

In sum, the results with the Prussian blue mediated electrodes showed 3-times higher sensitivity than the Cobalt phthalocyanine mediated ones. Besides, the measurement of the hydrogen peroxide takes place at 0 V *versus* 0.1 M Ag/AgCl in the case of PB mediated electrodes (while +0.4 V for CP mediated electrodes) which is very beneficial in order to exclude the oxidation of possible interfering substances at higher potentials. Therefore, the PB mediated carbon paste together with the curved electrode (design 2) were chosen for the final chip design.

Differential electrode design

The differential sensor design comprises two working electrodes on a single chip. One of these is the sensing electrode, containing PB as mediator and the other one consists of carbon paste without mediator serving as blank electrode to filter the background noise. Due to the similar resistance values of the carbon paste and the PB mediated paste, the current signal was expected to behave likewise and thus, signals coming from other sources than the oxidation of hydrogen peroxide could be easily excluded.

For the final paper based sensor with the differential electrode design, a calibration curve of H_2O_2, as illustrated in **Figure S6**, was carried out by amperometric measurements at a voltage of 0 V *versus* screen-printed Ag/AgCl (1 M). Here, H_2O_2 concentrations in a range between 5 and 160 µM delivered a linear current response with a sensitivity of 0.23 nA μM^{-1} mm^{-2} and a correlation coefficient of 0.99.

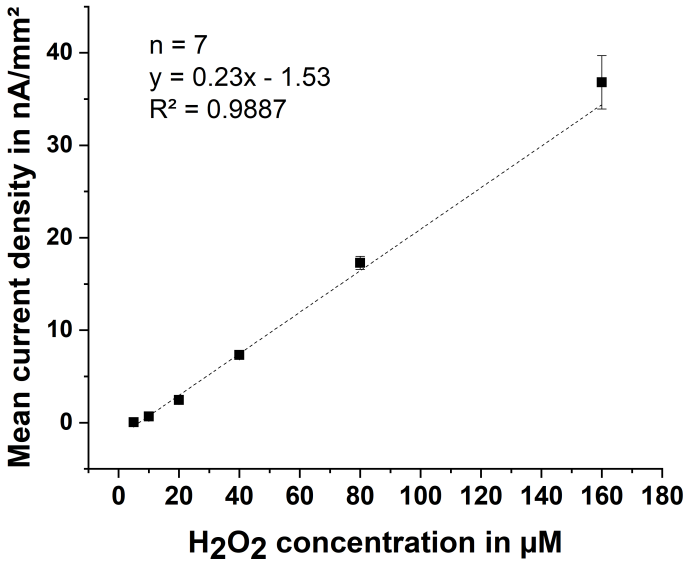

Figure S6. Calibration curve of differential electrode design for H_2O_2 concentrations between 5 and 160 µM in 1 M KCl solution applied to the front of the sensor chip. For this calibration, the whole 3D area of the working electrode is in contact with the sample solution. Error bars represent ± SD of n = 7 replicates.

System integration

To enable a comfortable use of the developed H_2O_2 sensor in on-site or clinical breath monitoring, it is supposed to be compatible with a common respiratory mask. For this purpose, the housing of a commercially available filter for anaesthetic applications (Ultipor® 25, Pall corporation, US) was modified. Herein, the filter was removed from the housing and the sidewalls were replaced by customized 3D printed sidewalls. These sidewalls were designed with SolidWorks 2017 (Dassault Systèmes, France), so that the chip fits airtight into the housing and the contact pads of the sensor are located on the outside. They were manufactured via 3D printing with the Ultimaker 3 Extended (Geldermalsen, The Netherlands).

Figure S7 shows an image of the respiratory mask with the extension containing the paper based H_2O_2 sensor. As paper itself is too vulnerable, it needs to be stabilized before the integration into the housing for the demonstrator version. Therefore, 1 mm thick poly(methyl methacrylate) (PMMA) sheets with a double sided adhesive film were lasered and the paper based sensors were placed in between two PMMA sheets. With these carriers, not only the stabilization of the paper based sensors is achieved, but also the conducting tracks are isolated against humidity, while an opening ensures that the electrodes are exposed to the breath (**Figure S7B**).

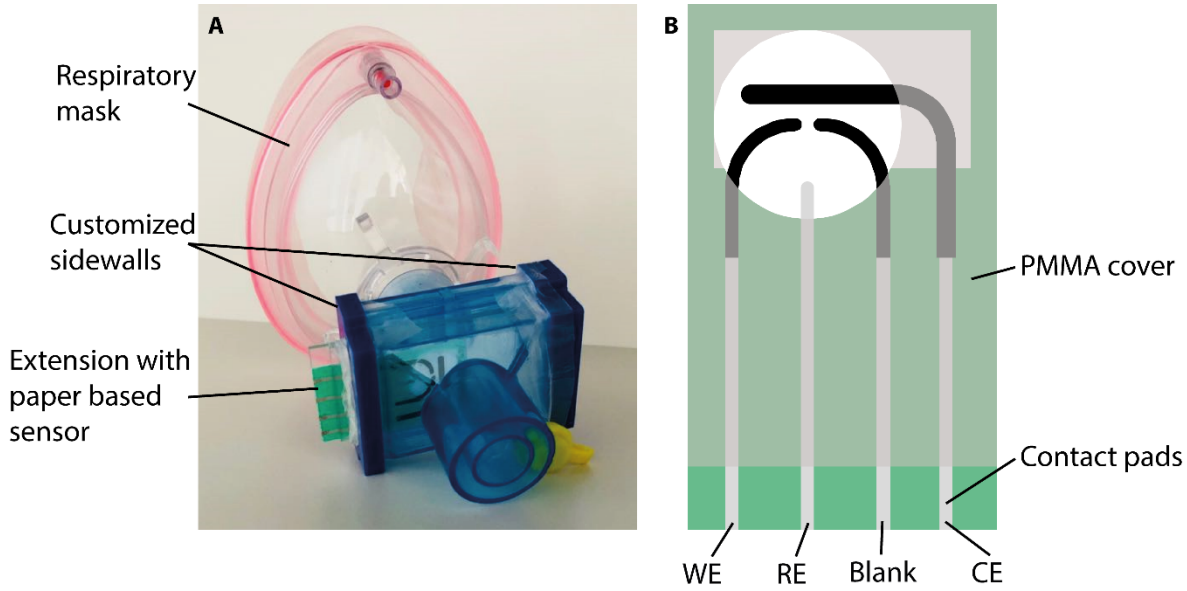

Figure S7. (A) Image of respiratory mask with extension with customized 3D printed sidewalls, containing the paper based H_2O_2 sensor and **(B)** CAD drawing of differential electrode design with a hydrogen peroxide sensing working electrode (WE), consisting of PB mediated carbon, a carbon blank electrode (Blank) to subtract background, a silver / silver chloride reference electrode (RE), a carbon counter electrode (CE) and a PMMA cover for stabilization and isolation of conducting tracks from humidity.

Electrochemically active electrode area

Due to the roughness of the paper substrate, the active surface area of the screen-printed electrodes could deviate largely from the geometric area. To examine the electrochemically active surface area, cyclic voltammograms of screen-printed carbon electrodes on both, paper and foil, were performed at different scan rates, between 25 and 200 mV s^{-1}. First, the capacitive contribution was determined in 50 mM KCl. Then, CVs in 1 mM ferrocenemethanol were recorded to identify the peak currents I_p for the reduction peaks at the different scan rates v. After subtracting the capacitive current signals, the mean values of the peak currents (n = 4) were plotted over the square root of the scan rate and the slope was determined to calculate the electrochemically active electrode area A. The results are shown in **Figure S8**. The relation between these variables is described in the rearranged Randles-Sevcik equation:

$$A = \frac{I_p}{v^{\frac{1}{2}}} \cdot (2.69 \cdot 10^5 \cdot n^{\frac{3}{2}} \cdot D^{\frac{1}{2}} \cdot c_0)^{-1}$$

with the number of transferred electrons n, the diffusion coefficient D of the electroactive species and the bulk concentration of the redox molecules c_0.

The ratio between the electrode areas on paper and foil was calculated by considering that the paper electrodes have a larger surface area. The assumption was that the foil blocks one whole side of the electrode and therefore, the area of the foil electrode only amounts 51% of the paper electrode area. However, taking this into account, the resulting experimental ratio of 0.959 implies, that the electrochemically active area on paper is insignificantly smaller than the one on foil. A possible reason might be that paper fibers block a part of the electrode surface and therewith, reduce its availability for the redox active species.

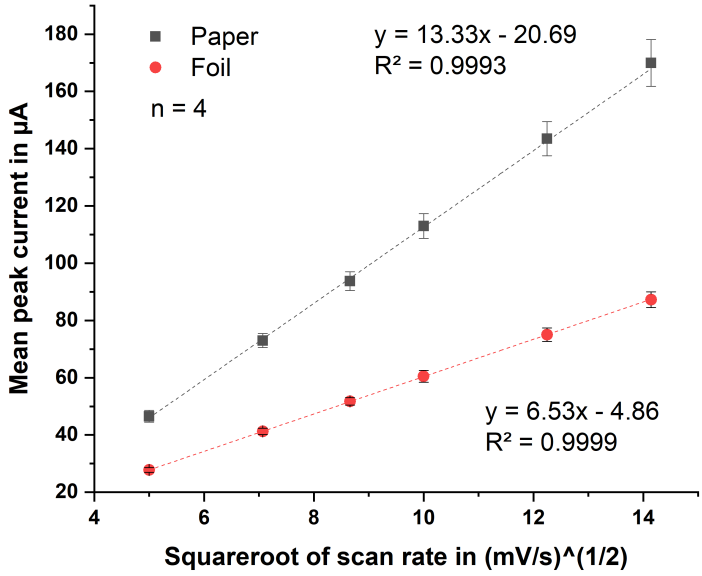

Figure S8. Plot of mean peak current over square root of scan rate for the screen-printed electrodes on paper and foil in order to determine the electrochemically active electrode area. Error bars represent ± SD of n = 4 replicates.

Study of different electrolytes

Since the paper itself is not well-conductive, it is necessary to treat the paper with electrolyte prior to an experiment. This was done by placing an electrolyte droplet onto the paper and allowing it to dry, before measuring in vapor. For the first measurements, 0.1M PBS was used, but during the measurement the sensor got dry quickly and it was not possible to assure constant conditions. To overcome this problem, several electrolytes and humectants were tested, regarding their sensing performance under dry and wet conditions. The used solutions include 1 M potassium chloride,10× PBS, 1 M sodium acetate (NaOAc), 1 M ammonium acetate (AA), 1 M monosodium phosphate, 10% glycerine in 1 M KCl (aq), 10% ethylene glycol in 1 M KCl (aq), 10% polyethylene glycol in 1 M KCl (aq). Each of these was applied to a sensor (100 µl) and left to dry for one day. Subsequently, CVs were recorded, first with the dry sensors, second the sensor was wetted with 50 µl of DI water and finally, a droplet of 200 µl 160 µM H_2O_2 was added.

It turned out that most of the tested solutions either could not keep the paper wet or inhibited the hydrogen peroxide signal. In terms of humidity, the sodium acetate solution delivered the best result, since the CVs for the pure electrolyte in dry (after one day) and wet state are the same, as illustrated in **Figure S9D**, but for the amperometric measurement of H_2O_2, no reliable current signal could be obtained. None of the other solutions showed remarkably better characteristics (**Figure S9A-I**). Still, CVs in 1 M KCl delivered better characteristics and results than 0.1 M PBS, as shown in **Figure S9A**. Furthermore, the amperometric measurement of H_2O_2 in 1 M KCl provided a better sensitivity than in 0.1 M PBS. Therefore, 1 M KCl was chosen as electrolyte for further experiments.

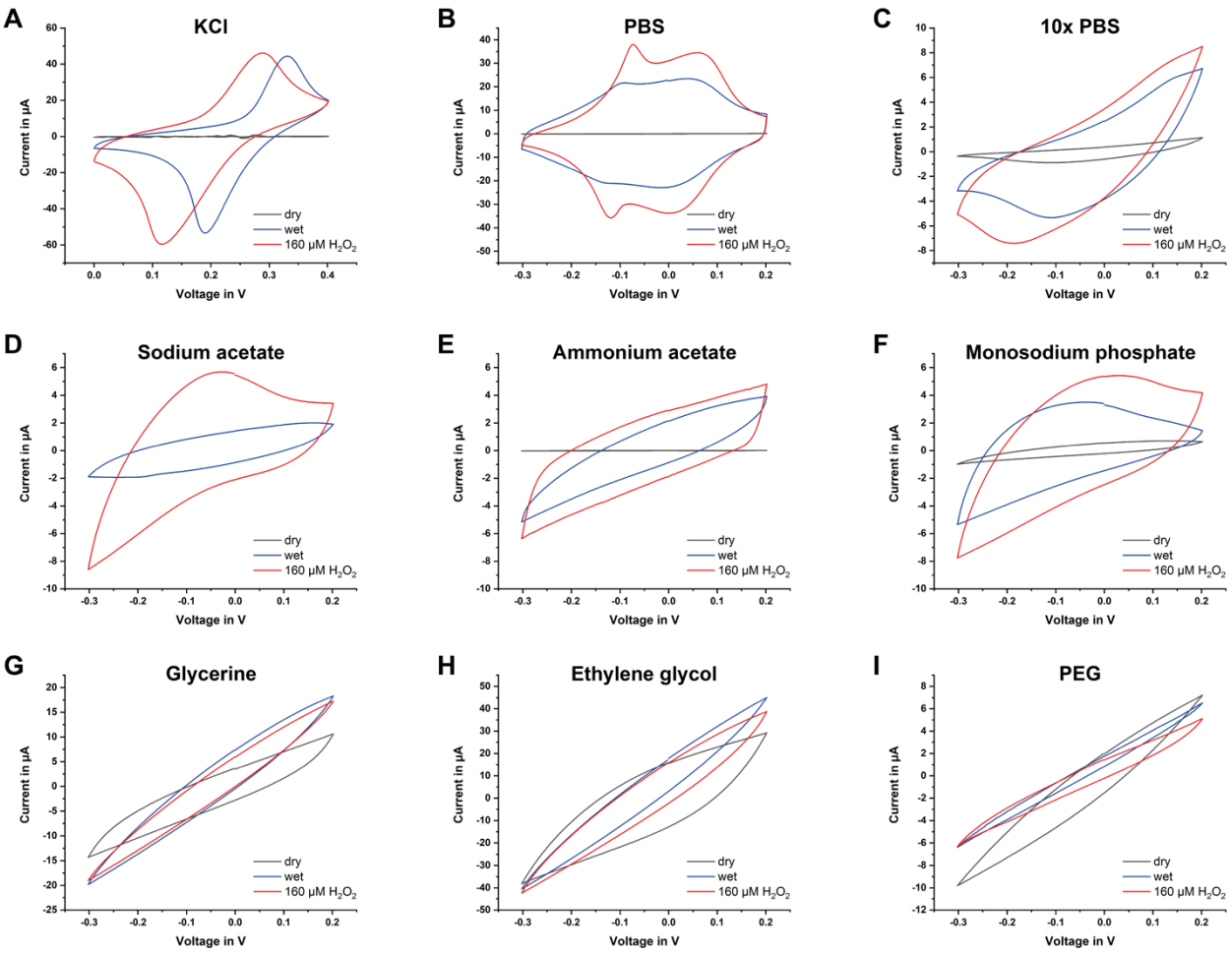

Figure S9. Cyclic voltammograms performed with chips under dry and wet condition and with 160 µM H_2O_2 at a scan rate of 200 mV s^{-1} in **(A)** 1 M KCl, **(B)** 0.1 M PBS, **(C)** 10× PBS, **(D)** 1 M sodium acetate, **(E)** 1 M ammonium acetate, **(F)** 1 M monosodium phosphate, **(G)** 10% glycerine in 1 M KCl, **(H)** 10% ethylene glycol in 1 M KCl and **(I)** 10% PEG in 1 M KCl. Please note that the results are given in current values, instead of current density, since the electrochemically active surface area of the dry sensor is undefined.

Stability of hydrogen peroxide solution

For evaporating hydrogen peroxide, a commercially available humidifier HME-BOOSTER® (Medisize, The Netherlands), consisting of a heater element, an intake for injecting the solution and an outlet for the vapor, was employed as shown in **Figure S10A**. During evaporation of hydrogen peroxide, diluted in a KCl solution, salt crystals formed, which blocked the pores of the humidifier. Therefore, from then on hydrogen peroxide was diluted in deionized water (DI water). This led to the problem, that lower current signals were observed. For this reason, the stability of H_2O_2 in DI water was studied and compared to H_2O_2 stability in 1 M KCl. Herein, amperometric measurements were performed with a fresh solution of H_2O_2 (10 minutes) and again after 90 minutes at 0 V (**Figure S10B**). As the stability *de facto* was worse in DI water than in 1 M KCl, but potassium chloride was crystallized in the evaporator, the compromise was to prepare the stock solution with 1 M KCl and then dilute the stock solution with DI water to the desired concentration immediately before evaporating.

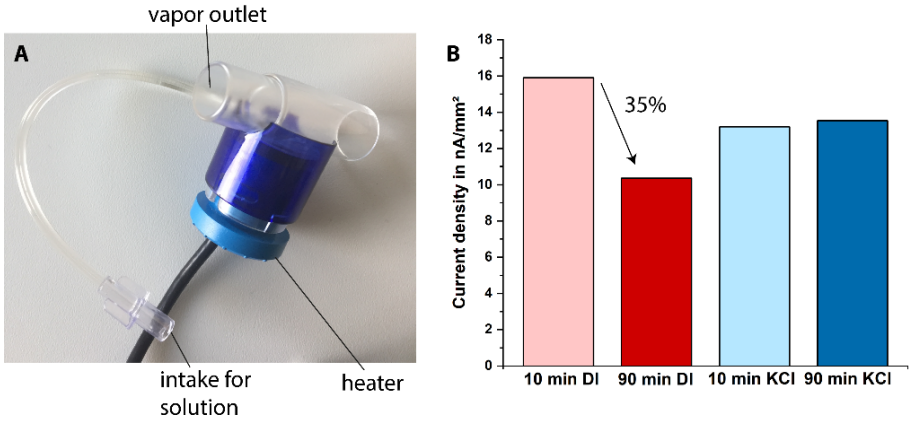

Figure S10. (A) Image of humidifier, used for hydrogen peroxide evaporation, with heater element, intake tube and vapor outlet and **(B)** resulting current densities of the stability tests with 80 µM hydrogen peroxide diluted in DI water and 1 M KCl after 10 and 90 min at 0.0 V *versus* Ag/AgCl, where for DI water a significantly higher decrease can be observed, than for potassium chloride.

Offset correction of measured current signals

As seen in **Figure 3C**, the measured current densities of blank and signal electrodes do not prove the same baseline, caused most probably due to the different composition of the employed pastes. However, this can be easily corrected by setting these signals to “zero” using an offset value prior to the measurement.

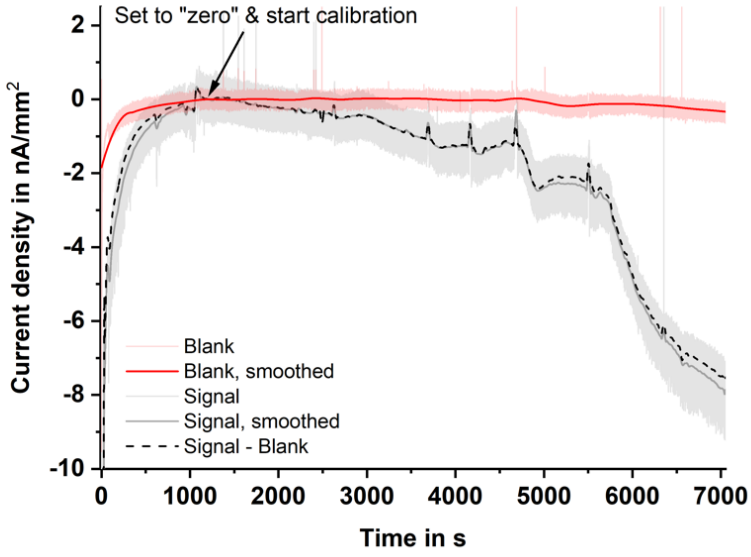

Figure S11. Offset corrected current density of a calibration measurement using 5 to 320 µM hydrogen peroxide in vapor.

Correlation of vaporous and aqueous H_2O_2 measurement

By division with a constant factor, a parallel linear plot (**Figure 3D**) can be obtained which is very close to the calibration curve in **Figure 2A**. Thus, it is very likely that the sensitivity of the sensor is exactly reproduced under the measuring conditions in the water-saturated vapor. Therefore, we assume that the paper based sensor shows exactly the same response with the same sensitivity as in solution. By adding a factor to the x values, the measured values in vapor can be superposed perfectly with the calibration curve. After this operation, the ratio between the original H_2O_2 concentrations of the prepared solutions used for the artificial breath and the obtained correlated concentrations are not completely conserved. For example, the ratio is 320:160 = 2 in aqueous, but only 42.91:22.73 = 1.89 in vapor. However, this is most probably caused by inaccuracies in the supply by the perfusor, and the evaporation would cause concentration fluctuations in the vapor. The optimization of the generation of artificial breath with accurately predefined H_2O_2 concentrations will be addressed in our future work.

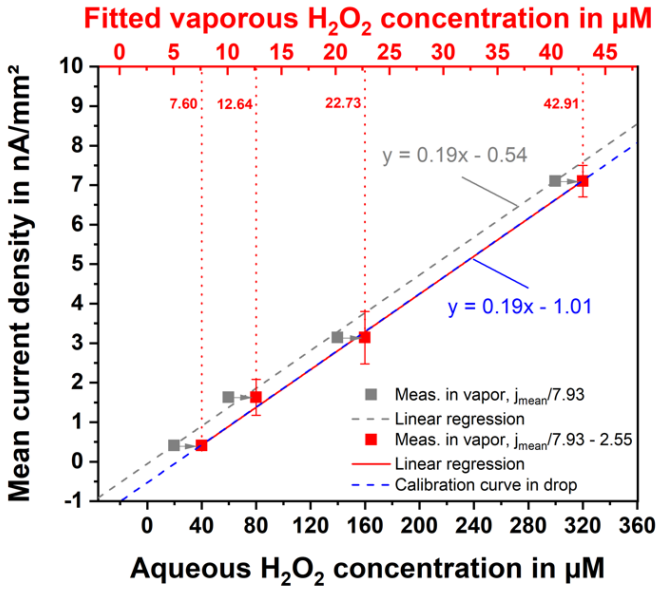

Figure S12. The detailed plot showing the correlation of the calibration curves of the aqueous and vaporous hydrogen peroxide measurement in artificial breath. Error bars represent ± SD of n = 3 replicates.

Measurement setup for simulated exhaled breath analysis

To demonstrate the applicability of the developed sensor for the exhaled breath analysis, a measurement setup was installed and human respiration was simulated. An image of this setup is illustrated in **Figure S13**. Furthermore, a video describing the measurement setup can be also found in the supporting information online.

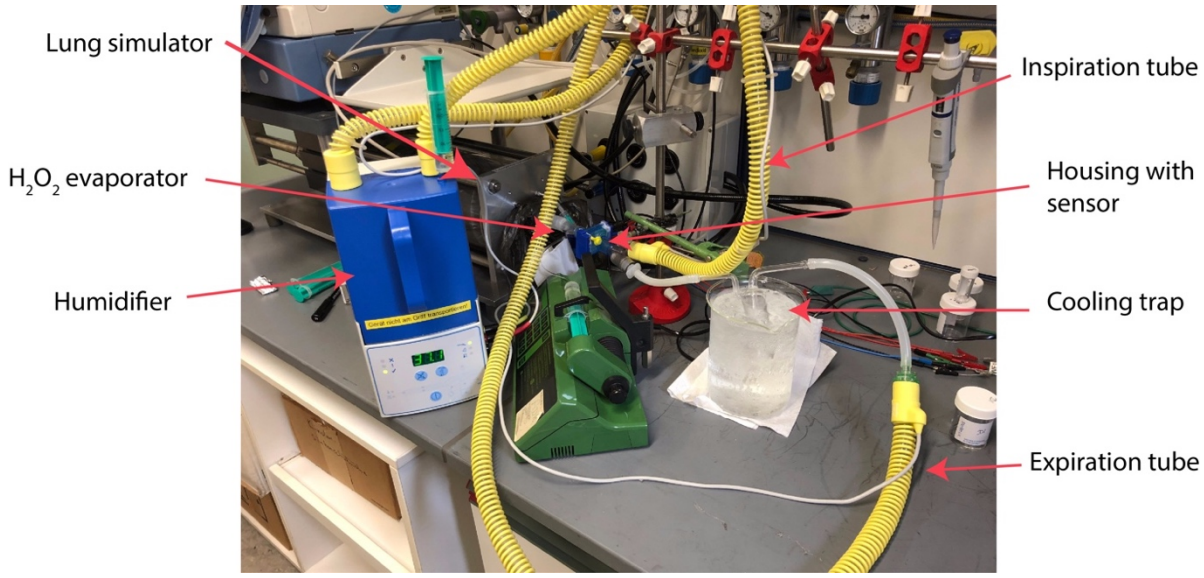

Figure S13. Image of measurement setup employed for exhaled breath analysis, including the lung simulator, the H_2O_2 evaporator, humidifier, heated inspiration and expiration tubes, the housing with the sensor and a cooling trap.

References

[1] Marinescu, M. and Winter, J., Grundlagenwissen Elektrotechnik: Gleich-, Wechsel- und Drehstrom. Vieweg+Teubner Verlag, **2011**.

Author Contributions

D.M., E.L. and C.D. designed the experiments. D.M. performed the experiments and analysed the data. A.B. performed the resistance measurements. D.M., E.L. and C.D. wrote the manuscript. E.L. and F.G. gave technical advice. C.D. conceived and managed the project and S.S., F.G. and G.U. supervised the work.